

Geometric properties of the additional third-order transitions in the two-dimensional Potts model

Xin Zhang^a, Wei Liu^{a,*}, Lei Shi^a, Fangfang Wang^{b,c,d}, Kai Qi^{e,*}, Zengru Di^{b,c,d}

^aCollege of Sciences, Xi'an University of Science and Technology, Xi'an, 710054, China

^bSchool of Systems Science, Beijing Normal University, Beijing, 100875, China

^cInternational Academic Center of Complex Systems, Beijing Normal University, ZhuHai, 519087, China

^dDepartment of Systems Science, Faculty of Arts and Sciences, Beijing Normal University, ZhuHai, 519087, China

^e2020 X-Lab, Shanghai Institute of Microsystem and Information Technology, Chinese Academy of Sciences, Shanghai, China

Abstract

Within the canonical ensemble framework, this paper investigates the presence of higher-order transition signals in the q -state Potts model (for $q \geq 3$), using two geometric order parameters: isolated spins number and the average perimeter of clusters. Our results confirm that higher-order transitions exist in the Potts model, where the number of isolated spins reliably indicates third-order independent transitions. This signal persists regardless of the system's phase transition order, even at higher values of q . In contrast, the average perimeter of clusters, used as an order parameter for detecting third-order dependent transitions, shows that for $q = 6$ and $q = 8$, the signal for third-order dependent transitions disappears, indicating its absence in systems undergoing first-order transitions. These findings are consistent with results from microcanonical inflection-point analysis, further validating the robustness of this approach.

Keywords: potts model, third-order transition, Swendsen-Wang Algorithm

1. Introduction

The Potts model [1, 2], a generalization of the Ising model [3, 4], has long been fundamental in statistical mechanics for studying phase transitions and critical phenomena in complex systems. Originally developed to explore magnetic properties [2], the Potts model has found applications across diverse fields, including optimizing communication networks like Wireless Body Area Networks and MESH networks [5]. Recent studies have expanded its scope to disciplines such as biophysics and statistical physics. For instance, Bae and Tai [6] introduced a four-phase Potts model for image segmentation, while Morcos et al. [7] applied it to protein structure prediction using direct coupling analysis. The model's relevance has recently been extended to machine learning, where Rende and colleagues [8] mapped the self-attention mechanism onto a generalized Potts model, demonstrating its effectiveness in solving the inverse Potts problem. These developments highlight the model's expanding interdisciplinary impact.

Traditional statistical physics and thermodynamics have been highly successful in explaining the behavior of phase transitions in systems. A phase transition is a cooperative phenomenon involving multiple factors such as temperature and pressure. The structure and properties of a system evolve in response to variations in certain order parameters, primarily temperature[9]. However, in the q -state Potts model ($q \geq 3$), when $q = 2$, the model reduces to the Ising model[2]. For $1 \leq q \leq 4$, the phase transition of the Potts model is continuous[10, 11], while for $q > 4$, the phase transition becomes discontinuous[11, 12, 13, 14, 15, 16, 17]. By incorporating bond percolation theory[18, 19, 20, 21], we can easily determine whether a phase transition is continuous or not. Percolation theory [22, 23, 24, 25] is the natural framework to study the properties of cluster-like structures of a system. Extensive research on percolation, especially focusing on both bond and site percolation in two and three dimensions, has

*Corresponding author

Email addresses: weiliu@xust.edu.cn (Wei Liu), kqi@mail.sim.ac.cn (Kai Qi)

been conducted, with significant contributions from Youjin Deng and his collaborators, covering critical transitions in percolation models [26, 27, 28, 29, 30]. As we know, the early warning of phase transitions hold theoretical significance and practical value [31, 32]. It raises the question of whether there exist abnormal behaviors that can act as precursors to the main phase transition.

Over the past few decades, microcanonical analysis has emerged as a valuable approach for identifying phase transitions in physical systems [33, 34]. Microcanonical inflection-point analysis (MIPA) has been recognized as an effective method for studying phase transitions in finite-size systems. Qi and Bachmann [35] expanded this approach to effectively identify higher-order transitions, distinguishing between independent and dependent transitions. The inflection point in a higher-order derivative of the microcanonical entropy specifically marks the point at which the monotonicity of the function changes, signaling the occurrence of a phase transition. Independent transitions, akin to conventional phase transitions, occur independently of other cooperative processes within the system. Dependent transitions, in contrast, are contingent upon the occurrence of lower-order transitions and take place at higher energy levels, representing higher-order phenomena.

Utilizing the exact density of states (DOS) of the Ising model [36], Sitarachu performed a comprehensive analysis of 1D and 2D finite-size Ising models, identifying higher-order transitions in the 2D system [37]. By using geometric order parameters in the canonical ensemble, Sitarachu et al. effectively demonstrated the correspondence between canonical and microcanonical ensemble methods for identifying third-order transitions [38]. Their analysis identified two forms of third-order phase transitions: independent and dependent transitions. The third-order independent transition occurs before the critical phase transition and is geometrically associated with the peak in the number of isolated spins, which disrupts the order of the system. This maximum is observed below the critical temperature. In contrast, the third-order dependent transition emerges beyond the critical point and is associated with a local minimum in the first derivative of the average cluster size with respect to temperature, indicating a shift in the decay rate of clusters in the disordered phase. This dependent transition is marked by a minimum above the critical temperature.

An important question arises: are these geometric signatures of third-order transitions universally applicable across different models? To address this, it becomes essential to test these methods on another model. This paper aims to explore the presence of third-order transition signals in the q -state Potts model (for $q \geq 3$). Through simulations in the canonical ensemble, we observed that applying the same geometric order parameters used in the Ising model to identify third-order transitions in the Potts model is not straightforward. In this work, we have redefined isolated spins and substituted the average cluster size with the average cluster perimeter. The rationale behind these modifications will be elaborated upon in the subsequent sections.

This paper is organized as follows: Section 2 introduces the Potts model and the Swendsen-Wang Algorithm, along with a detailed discussion on the third-order dependent phase transition observed in the system. Section 3 explores phase transitions, with Section 3.1 examining critical transitions—second-order for $q = 3$ and $q = 4$, and first-order for $q = 6$ and $q = 8$. Section 3.2 examines the third-order independent transition and the definition of isolated spins in the Potts model, while Section 3.3 details the use of the average perimeter as the order parameter for the third-order dependent transition. Section 4 concludes by discussing the results.

2. The model and method

2.1. Potts Model

The q -state Potts model [39], a generalization of the Ising model, is extensively utilized to study phase transitions in statistical mechanics. In this model, spins on a lattice may assume one of q discrete states, as opposed to the binary states in the Ising model. There is no external magnetic field in this model. The energy for a specific configuration of spins $X = (s_1, s_2, \dots, s_N)$, on a lattice with $N = L \times L$ sites, is expressed as:

$$E(X) = -J \sum_{\langle i, j \rangle} \delta(s_i, s_j) \quad (1)$$

where s_i represents the spin at site i , which may take values from 0 to $q-1$, and $\delta(s_i, s_j)$ is the Kronecker delta function, which equals 1 when $s_i = s_j$ and 0 otherwise. The summation is performed over all nearest-neighbor pairs $\langle i, j \rangle$, and $J > 0$ is the coupling constant that favors alignment of neighboring spins, reflecting ferromagnetic interactions. When $q = 2$, the Potts model reduces to the Ising model, while larger values of q lead to increasingly complex behavior and

phase transition dynamics. The model has been thoroughly investigated for its applications in understanding critical phenomena and phase transitions [11].

2.2. Swendsen-Wang Algorithm

It is well established [18] that the Potts model is intricately connected to problems of connectivity and percolation in graph theory. The Fortuin-Kasteleyn transformation [40] enables a mapping of the original model, which suffers from slow critical relaxation, into one where such relaxation effects are significantly mitigated. The transformation replaces each pair of interacting Potts spins on the lattice with a bond on an equivalent lattice with the probability:

$$p = 1 - e^{-K\delta_{\sigma_i, \sigma_j}}, \quad (2)$$

where $K = J/k_B T$, and $J = 1$. A bond is placed with probability p only when $\sigma_i = \sigma_j$, indicating that the spins of the nearest neighbors are in the same state. This implies that bonds are only formed with a non-zero probability when the corresponding pair of spins on the original lattice are in the same state. The process must be repeated for all pairs of spins, resulting in a lattice where bonds connect certain sites, forming clusters of varying sizes and shapes.

The first use of the Fortuin–Kasteleyn transformation in Monte Carlo simulations was made by Swendsen and Wang [41]. The process involves traversing the lattice and placing bonds between each pair of spins with the probability given by equation (2). The Hoshen–Kopelman [42] method is then employed to identify all clusters of sites connected by the bond network. Each cluster is subsequently assigned a new spin value from the set $q = \{0, 1, 2, \dots, q-1\}$, ensuring that all sites within a given cluster share the same randomly chosen spin value. This constitutes one Monte Carlo step in our algorithm. In the next Monte Carlo step, based on the spin configuration from the previous step, new bonds are re-established between neighboring spins according to the predefined probability. The Hoshen-Kopelman algorithm [42] is once again employed to identify clusters, after each cluster is reassigned a new spin value uniformly from the set $q = \{0, 1, 2, \dots, q-1\}$. This process repeats iteratively until the desired number of Monte Carlo steps is reached. It is important to note that in our algorithm, a dedicated array is used to store the bond states between spins. This array is reset at the start of each Monte Carlo step, ensuring that the bonding configuration is entirely refreshed, with no correlation to the previous step's bonds.

In our algorithm, we emphasize that during each Monte Carlo (MC) step, the Hoshen-Kopelman (H-K) algorithm is applied twice for cluster statistics: first to identify clusters within the system, followed by a spin-flipping process in which F-K clusters are defined by introducing a bond between two nearest-neighbor spins with identical orientations, based on the probability outlined in equation (2). However, once the F-K clusters are established, it is essential to ascertain the true physical state of the system to compute the order parameters accurately. This requires the formation of clusters solely from nearest-neighbor spins that share the same orientation after the spin-flipping operations, ensuring that the final cluster information aligns with the actual physical system. Thus, while the construction of F-K clusters addresses the issue of critical slowing down during spin flips, the accurate computation of physical quantities in the system necessitates considering the actual physical clusters present.

Since the probability of placing a bond between pairs of sites depends on temperature, it is clear that the resultant cluster distributions will vary dramatically with temperature. At very high temperatures, the clusters tend to be quite small. At very low temperatures, virtually all sites with nearest neighbors in the same state will end up in the same cluster, leading to oscillations between similar structures. Near the critical point, a diverse array of clusters emerges, resulting in each configuration differing significantly from its predecessor. This effectively reduces the phenomenon of critical slowing down. By employing the Swendsen-Wang (S-W) algorithm, the critical slowing down is significantly mitigated, facilitating faster convergence and more efficient sampling in Monte Carlo simulations [43].

If we aim to study the order of phase transitions, the F-K transformation is an effective tool for this purpose. In the F-K clusters, the probability of a randomly selected spin belonging to the largest cluster, denoted as $\langle P_\infty \rangle = \langle n_\infty \rangle / L^2$, where $\langle n_\infty \rangle$ represents the size of the largest cluster, shows behavior that is consistent with the magnetization $\langle M \rangle$ as calculated from real clusters when $T \leq T_c$ [44]. However, in the paramagnetic phase ($T > T_c$), discrepancies arise between these two quantities, as many clusters contribute to the magnetization $\langle M \rangle$, rather than solely the largest cluster, which is represented by $\langle P_\infty \rangle$. Fluctuation quantities, such as specific heat and susceptibility, exhibit related differences that arise from distinct contributions of clusters. In particular, one must separate the contributions from clusters smaller than the largest one and those from the size of the largest cluster itself [45]. To identify additional signals of higher-order phase transitions, especially in the paramagnetic phase, it is crucial to seek an alternative and appropriate order parameter that can more effectively capture subtle changes associated with these transitions [38].

2.3. Third-order transitions

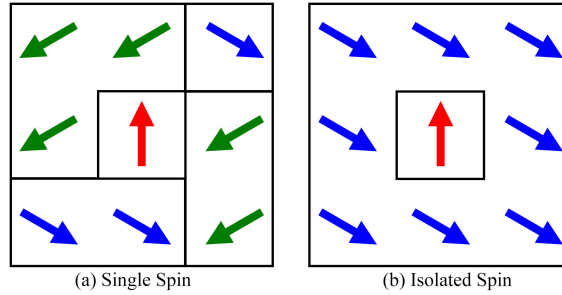


Figure 1: Comparison of Single Spins and Isolated Spins in the $q = 3$ state Potts model. Red represents $q = 0$, blue represents $q = 1$, and green represents $q = 2$. The figure illustrates the distinction between single spins, which differ from their nearest neighbors regardless of cluster membership, and isolated spins, which differ in orientation from their four nearest neighbors, all of which belong to the same cluster.

Microcanonical inflection-point analysis demonstrates the occurrence of a third-order independent transition before the critical phase transition. Geometrically, this third-order independent transition corresponds to a peak in the count of isolated spins, observed just before the phase transition. In the Ising model, the third-order transition is observed at $T_{in} \approx 2.229$ [38]. However, when applying the same definition of isolated spins from the Ising model to the Potts model, the number of isolated spins increases monotonically with temperature, without showing evidence of a third-order independent transition. This is because, in the q -state Potts model (for $q \geq 3$), spins can adopt more than two states. If isolated spins are defined solely based on having a different orientation from their four nearest neighbors, as depicted in Fig. 1 (a), their count will continue increasing monotonically with temperature, without showing any anomalous behavior indicative of a third-order independent transition.

Therefore, in the q -state Potts model (for $q \geq 3$), it is necessary to redefine the concept of isolated spins. In the Ising model, it is observed that, due to the nature of the system, an isolated spin is surrounded by four nearest neighbors that have the same orientation, which is opposite to that of the spin itself. This leads to the hypothesis that the role of an isolated spin is to serve as a disrupter of order within the system. Extending this logic to the q -state Potts model, isolated spins are similarly defined. In an ordered cluster, an isolated spin serves as a disrupter, with a different orientation from its four nearest neighbors, as shown in Fig. 1 (b), all of which belong to the same cluster. The isolated spin thus behaves like a "nail" driven into an ordered cluster, demonstrating its function as a source of disorder within an otherwise ordered system.

Microcanonical inflection-point analysis demonstrates that an additional third-order dependent transition occurs after the critical phase transition, occurring specifically within the paramagnetic phase, at a temperature distinct from the critical transition temperature. In the canonical ensemble, this corresponds to a slight shift in the rate at which the average cluster size decreases after the critical phase transition in the Ising model, specifically when $T > T_c$. Mathematically, this is identified by a local minimum in the first derivative of the average cluster size with respect to temperature. The temperature at which this minimum occurs indicates the occurrence of the third-order dependent transition, which, in the Ising model, is found to be $T_{de} \approx 2.567$ [38]. Following this logic, this approach is extended to the q -state Potts model (for $q \geq 3$) to search for the signal of a third-order dependent transition.

Subsequently, several order parameters were investigated in the q -state Potts model (for $q \geq 3$), and ultimately, the average perimeter size of clusters was identified as a key indicator for detecting the third-order dependent transition in the model. The process of identifying the average perimeter as an order parameter was somewhat unexpected. After realizing that the average cluster size could not pinpoint the third-order dependent transition in the q -state Potts model, an analysis of this parameter was conducted in detail. The average cluster size represents the average area of clusters, indicating the number of spins within each cluster. Since area failed to capture the signal, the focus was shifted to examining the average perimeter, which characterizes the number of spins on the boundary of each cluster, as shown in Fig. 2. Interestingly, during the analysis of the temperature dependence of the average perimeter, a similar trend was observed to that of the average cluster size in the 2D Ising model.

After identifying the average perimeter G as the order parameter for detecting the third-order dependent transition, the precise definition of the average perimeter, $\langle G \rangle$, is provided. G can be defined as the average perimeter of clusters

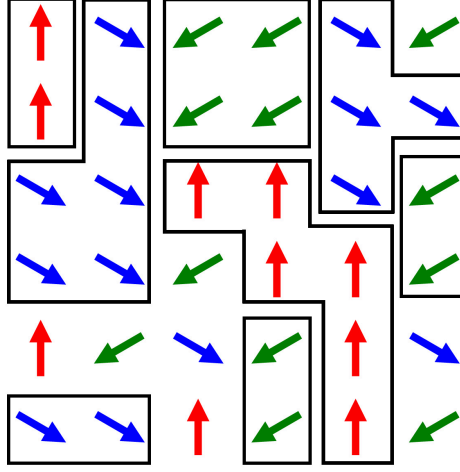


Figure 2: Cluster perimeter illustration for the $q = 3$ Potts Model. This figure demonstrates the relationship between cluster size and perimeter in the $q = 3$ Potts model. While the cluster size only indicates the number of spins within a cluster, the perimeter more accurately captures the boundary characteristics of the cluster. Clusters with the same number of spins can exhibit different configurations, resulting in distinct perimeters. This distinction makes the perimeter a more precise and effective metric for analyzing cluster configurations and identifying signals of higher-order phase transitions.

that contain more than one spin in a given spin configuration X :

$$G = \frac{1}{n} \sum_l P_l \quad (3)$$

where l labels the clusters with more than one spin, P_l is the perimeter of cluster l , and n is the total number of clusters with more than one spin in X . The statistical average is then obtained as:

$$\langle G \rangle = \frac{1}{Z} \sum_X G(X) e^{-E(X)/k_B T}, \quad (4)$$

where T is the canonical temperature and Z is the partition function defined as

$$Z = \sum_X \exp\left(-\frac{E(X)}{k_B T}\right). \quad (5)$$

3. Results and discussion

The following section discusses the results obtained from Swendsen-Wang spin-cluster simulations and cluster analysis to elucidate the system behavior associated with the additional transitions in the Potts model, as identified by microcanonical inflection-point analysis.

3.1. Critical transition

The primary goal of this paper is to determine the locations of both the third-order dependent and independent transitions in the q -state Potts model (for $q \geq 3$) for finite system sizes. The system sizes studied in this work are based on square lattices with edge lengths $L = 32, 64, 128, 256$. As derived by Wu [39], the exact solution for the critical transition temperature T_c of the q -state Potts model (for $q \geq 3$) is given by:

$$T_c = \frac{1}{\ln(1 + \sqrt{q})} \quad (6)$$

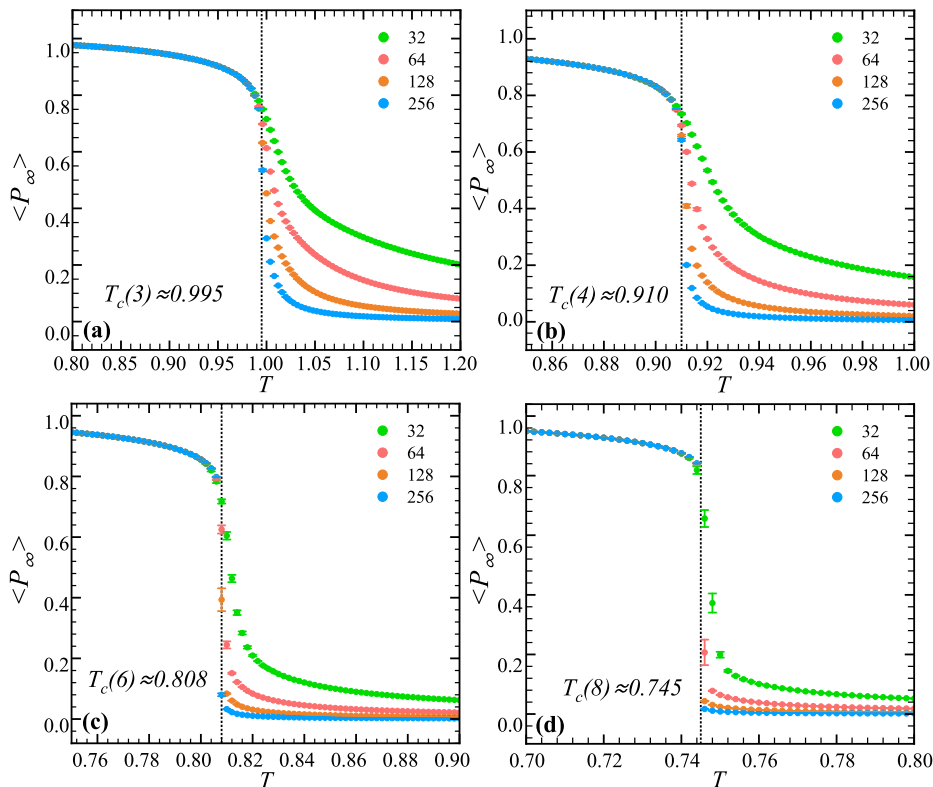


Figure 3: The variation of $\langle P_\infty \rangle$ with temperature is shown. The black dashed line marks the precise solution of the system's phase transition temperature T_c . As shown in panel (a) and (b), it is observed that at T_c , the $q = 3, 4$ Potts models exhibit characteristics of a continuous phase transition, indicating that the system undergoes a second-order phase transition for $q = 3, 4$. In contrast, in panel (c) and (d), for $q = 6, 8$, $\langle P_\infty \rangle$ shows a discontinuity at T_c , signifying that the system undergoes a first-order phase transition for $q = 6, 8$.

Therefore, for $q = 3, 4, 6$, and 8 , the corresponding critical transition temperatures approximate $T_c(3) \approx 0.995$, $T_c(4) \approx 0.910$, $T_c(6) \approx 0.808$, and $T_c(8) \approx 0.745$, respectively.

After identifying all the clusters in the system, various types of clusters emerge, and it is inevitable that the system contains a largest spin cluster. The proportion of spins in this largest cluster relative to the total system size, $\langle n_{\text{largest}}/L^2 \rangle$, defines the magnetization $\langle M \rangle$ in the ferromagnetic system [40]. By analyzing the behavior of $\langle M \rangle$, the order of the phase transition in the q -state Potts model (for $q \geq 3$) can be determined [46]. In Fig. 3 (a) and (b), it is observed that for $q = 3$ and $q = 4$, $\langle M \rangle$ changes continuously with temperature, which aligns with the results from Wu [39] and Baxter [11]. This confirms that the phase transitions in the q -state Potts model for $q = 3$ and $q = 4$ are critical, i.e., second-order phase transitions. For $q = 6$ and $q = 8$, $\langle M \rangle$ exhibits discontinuous behavior, consistent with the numerical simulation results reported in the existing literature [11, 13, 14, 15, 16, 17], indicating a first-order phase transition when $q = 6$ and $q = 8$.

3.2. Third-order independent transition in the ferromagnetic phase

As shown in Fig. 4 (a)-(d), the number of isolated spins in the $q = 3, 4, 6, 8$ Potts models, respectively, varies as a function of temperature. It is observed that the number of isolated spins initially increases with temperature, reaching a peak at $T_{\text{in}}(3) \approx 0.964$ for the 3-state Potts model, $T_{\text{in}}(4) \approx 0.880$ for the 4-state Potts model, $T_{\text{in}}(6) \approx 0.788$ for the 6-state Potts model, and $T_{\text{in}}(8) \approx 0.734$ for the 8-state Potts model. In Fig. 4, comparing the temperature of the third-order independent transition, T_{ind} , with the phase transition temperature, T_c , at the same q , the differences are approximately $\Delta T(3) \approx 0.031$, $\Delta T(4) \approx 0.030$, $\Delta T(6) \approx 0.020$, and $\Delta T(8) \approx 0.011$. It is evident that for $q = 3$ and $q = 4$, the third-order independent transition occurs at a notable distance from the critical transition, with $\Delta T(3) \approx \Delta T(4)$. However, for $q = 6$ and $q = 8$, ΔT starts to decrease, and as q increases, ΔT becomes smaller. Although the tem-

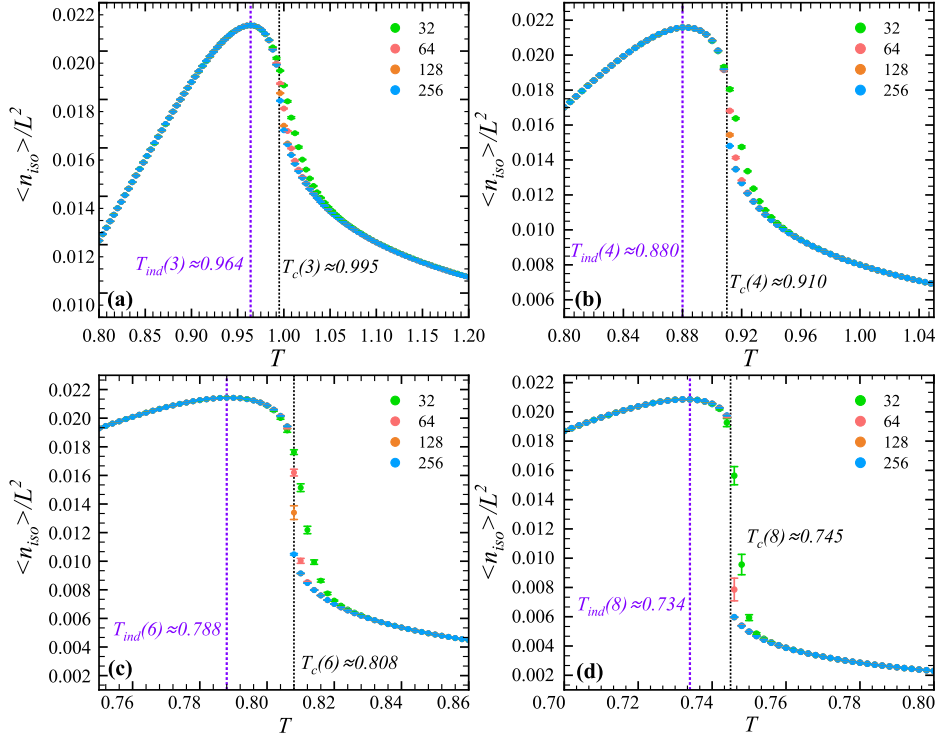


Figure 4: The variation of isolated spins (ISO) with temperature for $q = 3, 4, 6, 8$ is depicted in panels (a)-(d), respectively. The purple dashed line marks the temperature corresponding to the third-order independent transition, while the black dashed line indicates the precise solution of the system's phase transition temperature T_c . As shown in the figure, the temperatures corresponding to the third-order independent transition are identified as $T_{in}(3) = 0.964$, $T_{in}(4) = 0.88$, $T_{in}(6) = 0.788$, and $T_{in}(8) = 0.734$.

peratures of the third-order independent transition and the system's critical transition become closer, microcanonical inflection point analysis shows a re-entrant behavior of the inverse temperature as energy increases[47], meaning that a single temperature corresponds to two energy levels. Near $T = T_c$, the system exhibits a two-phase coexistence. Therefore, despite the proximity of these temperatures, there remains a distinct difference in the system's states.

As shown in Fig.5, it becomes apparent that at low temperatures ($T < T_c$), the largest cluster (LCS) dominates the system, nearly occupying the entire space, with little variation in its size and configuration. Prior to the phase transition, the percolation cluster continues to dominate, oscillating between similar structures. Disrupting the LCS at low temperatures can be achieved by isolated spins with orientations different from those within the LCS. During the spin-flip process, the LCS has a probability $P = 1 - e^{-K}$ of being flipped, where $K = J/(k_B T)$, resulting in changes to the required isolated spin states. As temperature increases, more clusters form, leading to an increase in the number of isolated spins of various types. In the paramagnetic phase at high temperatures, the system becomes highly disordered, with more clusters appearing. Panels (a)-(d) show the variation of isolated spins with temperature: $T(a) = T(e) = 0.8$, $T(b) = T(f) \approx T_{in} \approx 0.964$, $T(c) = T(g) \approx T_c \approx 0.995$, and $T(d) = T(h) \approx T_{de} \approx 1.06$. The number of isolated spins reaches a maximum at T_{ind} and then decreases as temperature increases further, while the number of single spins rises continuously, indicating increasing disorder in the system.

Considering an arbitrary value of q , it is observed that for different system sizes L , the behavior of $\langle n_{iso} \rangle / L^2$ as a function of temperature remains consistent. That is, for the same value of q , the proportion of isolated spins to the system size L^2 remains invariant across different system sizes. Based on this, it is hypothesized that if the system is divided into several uniform regions, the isolated spins dominate each region. Once an isolated spin appears in a region, the probability of another isolated spin appearing in the same region decreases, and new isolated spins are more likely to appear in previously unoccupied regions. When all regions are occupied by isolated spins, the number of isolated spins reaches its maximum. As the temperature increases, isolated spins tend to reappear in regions where they have already emerged. These newly formed isolated spins merge with the existing ones, forming new clusters,

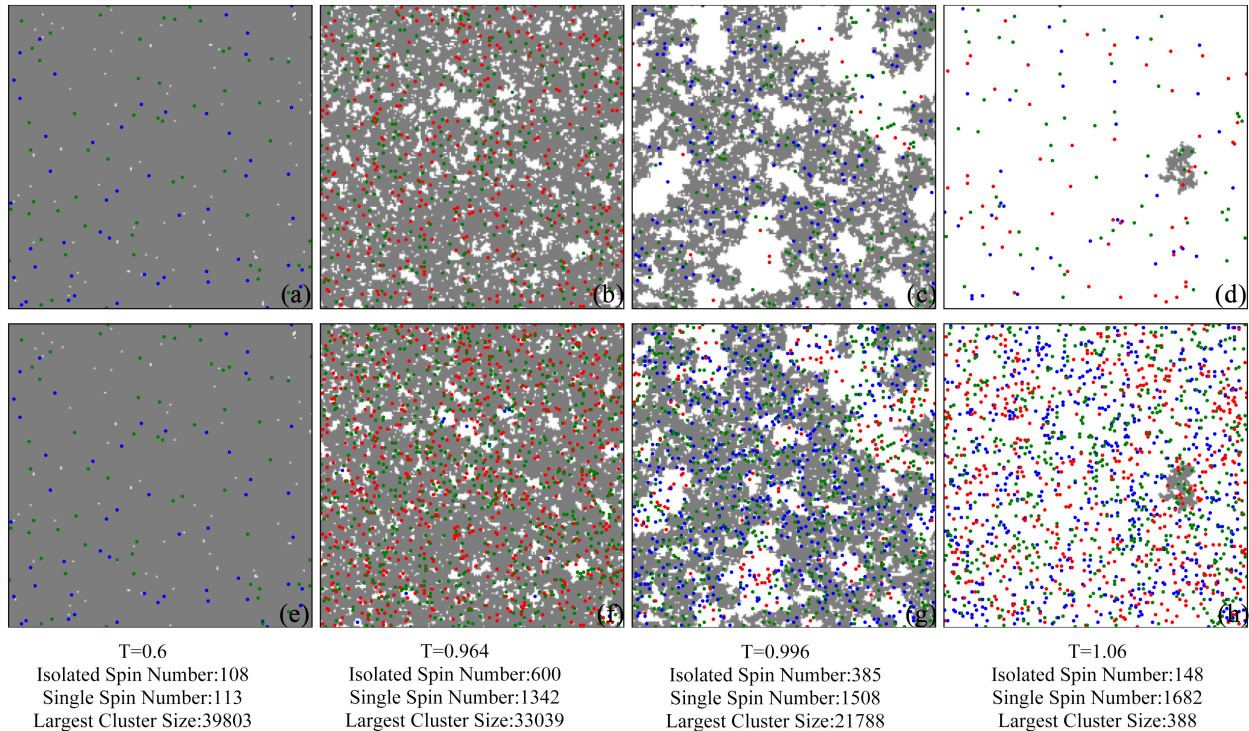


Figure 5: A comparison of isolated spins (ISO) and single spins in the $q = 3$ Potts model is provided on a lattice with $N = 200 \times 200$. In the figure, the largest cluster size(LCS) in the system is shaded in gray, while all other clusters containing more than two spins are depicted in white, regardless of their spin orientations. The red points represent spins with $s_i = 0$, the green points represent $s_i = 1$, and the blue points represent $s_i = 2$.

which explains the subsequent decrease in the number of isolated spins.

The extremum of $\langle n_{\text{iso}} \rangle / L^2$ is examined for different values of q : $\langle n_{\text{iso}}(3) \rangle / L^2 \approx \langle n_{\text{iso}}(4) \rangle / L^2 \approx \langle n_{\text{iso}}(6) \rangle / L^2 \approx \langle n_{\text{iso}}(8) \rangle / L^2 \approx 0.0215$. This is reasonable because, at $T < T_c$, the percolation cluster remains dominant, and in a square lattice system, the size and configuration of the percolation cluster are similar across different values of q . Hence, the proportion of isolated spins required to break the percolation cluster is nearly the same. This also explains why the third-order independent phase transition does not depend on the order of the system's phase transition and is consistently present.

Finally, an explanation is provided for why the temperature associated with the third-order dependent phase transition decreases as q increases. By referring to equation (2) and the SW algorithm, along with Fig. 5, it is noted that when a region is to generate an isolated spin, its spin orientation must differ from that of the percolation cluster. For smaller values of q , such as $q = 3$, an isolated spin has only two alternative spin orientations, with the third option being reintegration into the percolation cluster. In this case, the probability that a spin becomes isolated is $2/3$, requiring more energy to induce a spin variation. However, for $q = 8$, the situation is different. The probability that a spin becomes isolated increases to $7/8$, significantly reducing the energy required. Consequently, the temperature at which isolated spins reach their extremum decreases as q increases.

3.3. Third-order dependent transition in the paramagnetic phase

Fig. 6 illustrates the temperature dependence of the average perimeter $\langle G \rangle$ for the three-state and four-state Potts models. The first row displays the variation of the average perimeter $\langle G \rangle$ with temperature, exhibiting a backbending pattern analogous to that observed in the Ising model. In Fig. 6 (c) and (d), it is observed that $d\langle G \rangle / dT$ exhibits a peak, and as the system size increases, the peak of $d\langle G \rangle / dT$ approaches the system's critical temperature T_c , for both $q = 3$ and $q = 4$. Following this, after T_c , a minimum is observed in the variation of $d\langle G \rangle / dT$ with temperature, as shown in Fig. 6 (c) and (d). The temperature at which this minimum occurs corresponds to the system's third-order

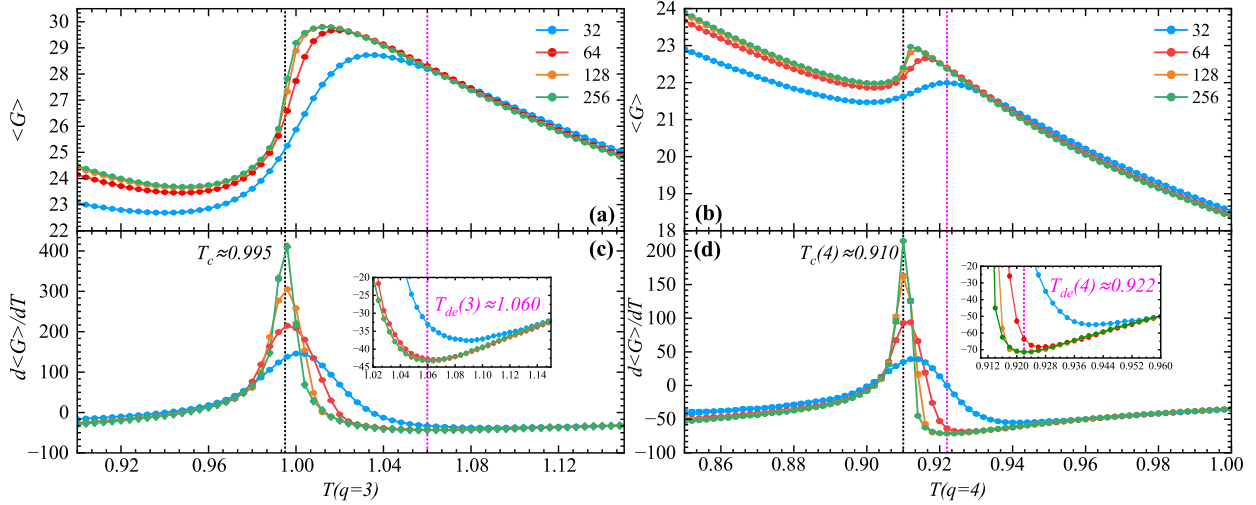


Figure 6: Panels (a) and (b) show the variation of the average perimeter $\langle G \rangle$ with temperature for $q = 3, 4$, while panels (c) and (d) depict the first derivative of the average perimeter with respect to temperature, $d\langle G \rangle/dT$. The black dashed line represents the exact solution for the phase transition temperature of the corresponding q -state Potts model. For any value of q , it is observed that as L increases, the location of the maximum in $d\langle G \rangle/dT$ approaches the phase transition temperature. The pink line indicates the location of the third-order dependent transition temperature, with $T_{de}(3) \approx 1.06$ and $T_{de}(4) \approx 0.922$.

transition temperature, and these results align with those obtained through microcanonical inflection-point analysis [47].

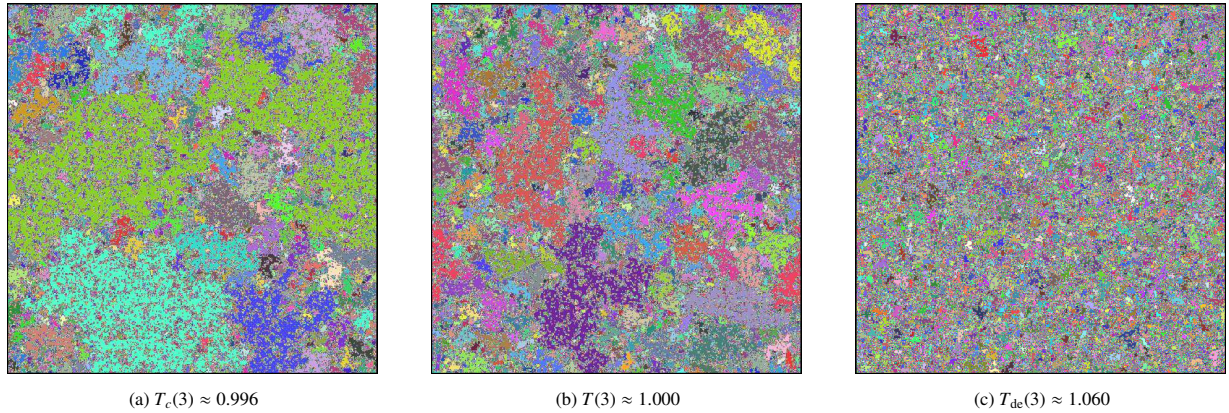


Figure 7: Clusters identified in typical spin configurations on the 500×500 lattice for $q = 3$ at three different temperatures: (a) $T \approx 0.996$, is the critical temperature. (b) $T \approx 1.000$, just above the critical temperature, is approaching third dependent transition temperature. (c) $T \approx 1.060$, is the third dependent transition temperature.

By comparing the average perimeter results for the three-state and four-state Potts models in Fig. 6 (a) and (b), we observe a noteworthy phenomenon: the average perimeter $\langle G \rangle$ exhibits a local minimum prior to the critical phase transition and a local maximum subsequent to the transition. The maximum is referred to as the "peak," whereas the minimum is designated as the "valley." The difference between the peak and the valley is termed the "height difference." It is evident that as q increases in the q -state Potts model (for $q \geq 3$), this height difference diminishes significantly. This observation reflects the behavior of clusters within the system under varying q -state conditions. As q increases, the boundary conditions of the clusters become smoother, resulting in a simplification of the fractal structure. In Fig. 6 (c) and (d), it is observed that $d\langle G \rangle/dT$ exhibits a local minimum. The temperature corresponding to this minimum is identified as the temperature T_{de} associated with the third-order dependent transition. This minimum

indicates that, within a temperature range T prior to T_{de} , the average perimeter decreases as a concave function with increasing temperature; conversely, after T_{de} , it decreases as a convex function. Therefore, T_{de} marks the inflection point at which the concavity of the average perimeter as a function of temperature changes, signifying the location of the third-order dependent transition. To gain a more intuitive understanding of the cluster information within the system, we simulated the clusters in the $q = 3$ Potts model at three distinct temperatures: $T_c(3) \approx 0.996$, $T(3) \approx 1.000$, and $T_{de}(3) \approx 1.060$, as shown in Fig. 7.

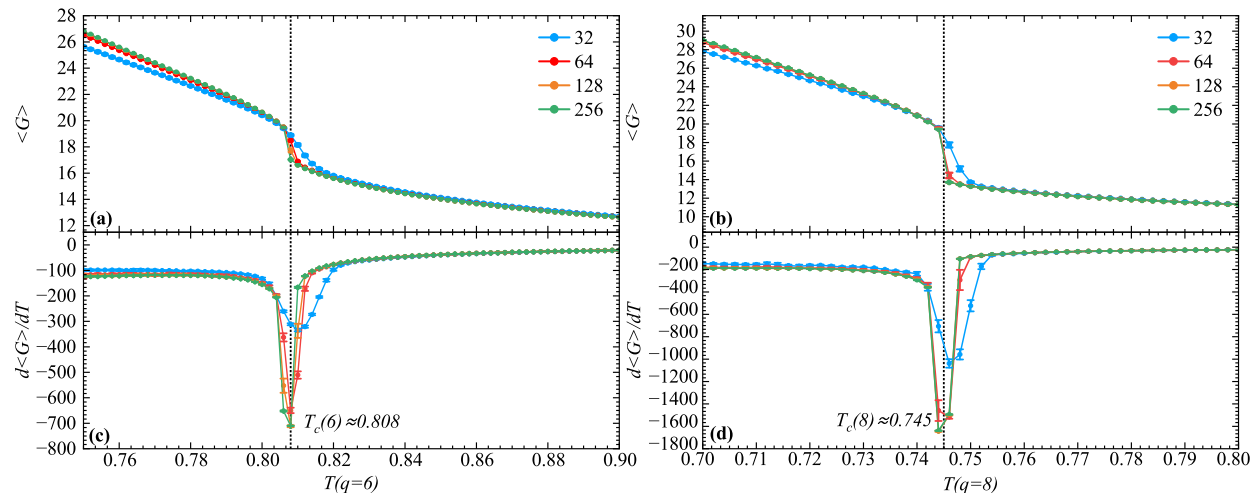


Figure 8: Panels (a) and (b) show the variation of the average perimeter $\langle G \rangle$ with temperature for $q = 6, 8$, while panels (c) and (d) depict the first derivative of the average perimeter with respect to temperature, $d\langle G \rangle/dT$. The black dashed line represents the exact solution for the phase transition temperature of the corresponding q -state Potts model. For any value of q , it is observed that as L increases, the location of the minimum in $d\langle G \rangle/dT$ approaches the phase transition temperature. This minimum is not a signal of a third-order dependent transition, but rather indicates that as q increases, the average perimeter $\langle G \rangle$ decreases with temperature, lacking any additional phase transition signals.

In Fig. 8 (a) and (b), it is observed that the average perimeter $\langle G \rangle$ decreases as the temperature increases. Although the first derivative $d\langle G \rangle/dT$ exhibits a minimum, as shown in Fig. 8 (c) and (d), it is evident that this minimum shifts closer to the system's critical temperature T_c as the system size increases, without indicating a signal of a third-order dependent transition. Previously, the order of the phase transition was determined by analyzing the relationship between $\langle P_\infty \rangle$ and $\langle M \rangle$, as shown in Fig. 3. For $q = 6$ and $q = 8$, the system undergoes a first-order phase transition. Based on this, it is speculated that no third-order dependent transition signals exist in systems undergoing first-order transitions. In contrast, for $q = 3$ and $q = 4$, where the system exhibits a continuous phase transition, third-order dependent transition signals are present.

To further investigate the suitability of the average perimeter $\langle G \rangle$ as an order parameter, calculations were also performed for the Ising model. Notably, the temperature at which the average perimeter changes is slightly higher than the temperature corresponding to the third-order dependent transition when calculated using the average cluster size. However, the difference between the two temperatures is not significant. This discrepancy could be attributed to the unique two-state nature of the Ising model, in which noise in the canonical ensemble may lead to such variations between the two methods.

4. Conclusion

This study establishes the existence of third-order phase transitions in the Potts model from a geometric perspective and identifies the positions of both the third-order dependent and independent transitions using two key order parameters: isolated spins and the average perimeter. Comparisons between the microcanonical inflection points and transition positions determined by specific heat under canonical conditions show strong agreement. Additionally, by analyzing the relationship between the largest Cluster Size (LCS) and the magnetization $\langle M \rangle$, the order of phase transitions was identified for different values of q . The results show that for $q = 3$ and $q = 4$, the system

undergoes continuous (second-order) transitions, accompanied by a third-order dependent transition. However, when $q = 6$ and $q = 8$, the system exhibits discontinuous (first-order) transitions, where the third-order dependent transition vanishes. Regardless of the value of q , a third-order independent transition persists, serving as a precursor to the impending disruption of the system's highly ordered state. This comprehensive investigation validates the robustness of these geometric order parameters in detecting higher-order transitions in complex systems, further enhancing our understanding of the intricate behavior of the Potts model across varying conditions.

5. Acknowledgments

We would like to thank Professor Ying Tang for his valuable discussion. This work is supported by the National Natural Science Foundation of China (Grant No.12304257).

References

- [1] R. B. Potts, Some generalized order-disorder transformations, in: *Mathematical proceedings of the cambridge philosophical society*, Vol. 48, Cambridge University Press, 1952, pp. 106–109.
- [2] F. Wu, Potts model of magnetism, *Journal of Applied Physics* 55 (6) (1984) 2421–2425.
- [3] L. Onsager, Crystal statistics. i. a two-dimensional model with an order-disorder transition, *Physical Review* 65 (3-4) (1944) 117.
- [4] S. G. Brush, History of the lenz-ising model, *Reviews of modern physics* 39 (4) (1967) 883.
- [5] A. Paszkiewicz, J. Węgrzyn, Responsiveness of the sensor network to alarm events based on the potts model, *Sensors* 20 (23) (2020) 6979.
- [6] X. Tai, L. Li, E. Bae, The potts model with different piecewise constant representations and fast algorithms: a survey, in: *Handbook of Mathematical Models and Algorithms in Computer Vision and Imaging: Mathematical Imaging and Vision*, Springer, 2023, pp. 1–41.
- [7] F. Morcos, A. Pagnani, B. Lunt, A. Bertolino, D. S. Marks, C. Sander, R. Zecchina, J. N. Onuchic, T. Hwa, M. Weigt, Direct-coupling analysis of residue coevolution captures native contacts across many protein families, *Proceedings of the National Academy of Sciences* 108 (49) (2011) E1293–E1301.
- [8] R. Rende, F. Gerace, A. Laio, S. Goldt, Mapping of attention mechanisms to a generalized potts model, *Physical Review Research* 6 (2) (2024) 023057.
- [9] R. K. Pathria, *Statistical Mechanics*, Elsevier(Singapore) Pte Ltd., 2001.
- [10] H. Duminił-Copin, V. Sidoravicius, V. Tassion, Continuity of the phase transition for planar random-cluster and potts models with $1 \leq q \leq 4$, *Communications in Mathematical Physics* 349 (2017) 47–107.
- [11] R. J. Baxter, Potts model at the critical temperature, *Journal of Physics C: Solid State Physics* 6 (23) (1973) L445.
- [12] H. Duminił-Copin, M. Gagnebin, M. Harel, I. Manolescu, V. Tassion, Discontinuity of the phase transition for the planar random-cluster and potts models with $q > 4$, in: *Annales scientifiques de l'École Normale Supérieure*, Vol. 54, Société Mathématique de France, 2021, pp. 1363–1413.
- [13] F. Iglói, E. Carlon, Boundary and bulk phase transitions in the two-dimensional q -state potts model ($q > 4$), *Physical Review B* 59 (5) (1999) 3783.
- [14] C. Hamer, Q -state potts models in hamiltonian field theory for $q \geq 4$ in $(1+1)$ dimensions, *Journal of Physics A: Mathematical and General* 14 (11) (1981) 2981.
- [15] F. Iglói, J. Sólyom, First-order transition for the $(1+1)$ -dimensional $q \geq 4$ potts model from finite lattice extrapolation, *Journal of Physics C: Solid State Physics* 16 (15) (1983) 2833.
- [16] M. P. Loureiro, J. J. Arenzon, L. F. Cugliandolo, A. Sicilia, Curvature-driven coarsening in the two-dimensional potts model, *Physical Review E—Statistical, Nonlinear, and Soft Matter Physics* 81 (2) (2010) 021129.
- [17] M. P. Loureiro, J. J. Arenzon, L. F. Cugliandolo, Geometrical properties of the potts model during the coarsening regime, *Physical Review E—Statistical, Nonlinear, and Soft Matter Physics* 85 (2) (2012) 021135.
- [18] C. M. Fortuin, P. W. Kasteleyn, On the random-cluster model: I. introduction and relation to other models, *Physica* 57 (4) (1972) 536–564.
- [19] M. Stephen, Percolation problems and the potts model, *Physics Letters A* 56 (3) (1976) 149–150.
- [20] F. Wu, Percolation and the potts model, *Journal of Statistical Physics* 18 (2) (1978) 115–123.
- [21] D.-S. Lee, K.-I. Goh, B. Kahng, D. Kim, Scale-free random graphs and potts model, *Pramana* 64 (2005) 1149–1159.
- [22] D. Stauffer, A. Aharony, *Introduction to percolation theory*, Taylor & Francis, 2018.
- [23] G. R. Grimmett, Inequalities and entanglements for percolation and random-cluster models, *Perplexing Problems in Probability: Festschrift in Honor of Harry Kesten* (1999) 91–105.
- [24] J. W. Essam, Percolation theory, *Reports on progress in physics* 43 (7) (1980) 833.
- [25] A. A. Saberi, Recent advances in percolation theory and its applications, *Physics Reports* 578 (2015) 1–32.
- [26] J. Wang, Z. Zhou, W. Zhang, T. M. Garoni, Y. Deng, Bond and site percolation in three dimensions, *Physical Review E—Statistical, Nonlinear, and Soft Matter Physics* 87 (5) (2013) 052107.
- [27] X. Feng, Y. Deng, H. W. Blöte, Percolation transitions in two dimensions, *Physical Review E—Statistical, Nonlinear, and Soft Matter Physics* 78 (3) (2008) 031136.
- [28] Y. Deng, H. W. Blöte, Simultaneous analysis of several models in the three-dimensional ising universality class, *Physical Review E* 68 (3) (2003) 036125.
- [29] Y. Deng, H. W. Blöte, Monte carlo study of the site-percolation model in two and three dimensions, *Physical Review E—Statistical, Nonlinear, and Soft Matter Physics* 72 (1) (2005) 016126.

- [30] X. Xu, J. Wang, J.-P. Lv, Y. Deng, Simultaneous analysis of three-dimensional percolation models, *Frontiers of Physics* 9 (2014) 113–119.
- [31] M. Scheffer, J. Bascompte, W. A. Brock, V. Brovkin, S. R. Carpenter, V. Dakos, H. Held, E. H. Van Nes, M. Rietkerk, G. Sugihara, Early-warning signals for critical transitions, *Nature* 461 (7260) (2009) 53–59.
- [32] M. F. Freeman, M. J. CG, Helf, brandon i. morinaka, agustinus r. uria, neil j. oldham, hans-georg sahl, shigeki matsunaga, jörn piel, metagenome mining reveals polytheonamides as posttranslationally modified ribosomal peptides, *Science* 338 (2012) 6105.
- [33] D. H. Gross, *Microcanonical thermodynamics: phase transitions in "small" systems*, Vol. 66, World Scientific, 2001.
- [34] C. Junghans, M. Bachmann, W. Janke, Microcanonical analyses of peptide aggregation processes, *Physical review letters* 97 (21) (2006) 218103.
- [35] K. Qi, M. Bachmann, Classification of phase transitions by microcanonical inflection-point analysis, *Physical review letters* 120 (18) (2018) 180601.
- [36] P. D. Beale, Exact distribution of energies in the two-dimensional ising model, *Physical Review Letters* 76 (1) (1996) 78.
- [37] K. Sitarachu, R. K. Zia, M. Bachmann, Exact microcanonical statistical analysis of transition behavior in ising chains and strips, *Journal of Statistical Mechanics: Theory and Experiment* 2020 (7) (2020) 073204.
- [38] K. Sitarachu, M. Bachmann, Evidence for additional third-order transitions in the two-dimensional ising model, *Physical Review E* 106 (1) (2022) 014134.
- [39] F.-Y. Wu, The potts model, *Reviews of modern physics* 54 (1) (1982) 235.
- [40] P. W. Kasteleyn, C. Fortuin, Phase transitions in lattice systems with random local properties, *Journal of the Physical Society of Japan Supplement* 26 (1969) 11–14.
- [41] R. H. Swendsen, J.-S. Wang, Nonuniversal critical dynamics in monte carlo simulations, *Physical review letters* 58 (2) (1987) 86.
- [42] J. Hoshen, R. Kopelman, Percolation and cluster distribution. i. cluster multiple labeling technique and critical concentration algorithm, *Physical Review B* 14 (8) (1976) 3438.
- [43] M. E. Newman, G. T. Barkema, *Monte Carlo methods in statistical physics*, Clarendon Press, 1999.
- [44] M. D. De Meo, D. W. Heermann, K. Binder, Monte carlo study of the ising model phase transition in terms of the percolation transition of "physical clusters", *Journal of statistical physics* 60 (1990) 585–618.
- [45] D. Landau, K. Binder, *A guide to Monte Carlo simulations in statistical physics*, Cambridge university press, 2021.
- [46] R. J. Baxter, *Exactly solved models in statistical mechanics*, Elsevier, 2016.
- [47] F. Wang, W. Liu, J. Ma, K. Qi, Y. Tang, Z. Di, Exploring transitions in finite-size potts model: comparative analysis using wang–landau sampling and parallel tempering, *Journal of Statistical Mechanics: Theory and Experiment* 2024 (9) (2024) 093201.